Magnetoelectric Coupling in $BaTiO_3$–$CoFe_2O_4$ Nanocomposites Studied by Impedance Spectroscopy Under Magnetic Field

René Lopez Noda[1,2], Ulises Acevedo Salas[2], Thomas Gaudisson[3], Francisco Calderón Piñar[4], Souad Ammar[3], and Raúl Valenzuela[2]

[1]Instituto de Cibernética, Matemática y Física, Universidad de La Habana, La Habana 10400, Cuba
[2]Instituto de Investigaciones en Materiales, Universidad Nacional Autónoma de México, México DF 04510, México
[3]ITODYS, Université Paris Diderot, PRES Sorbonne Paris Cité, Paris 75205, France
[4]Instituto de Ciencia y Tecnología de Materiales, Universidad de La Habana, La Habana 10400, Cuba

$BaTiO_3$–$CoFe_2O_4$ nanocomposites with a 1/1 molar ratio were prepared by a combination of polyol synthesis (chimie douce) and a subsequent consolidation by spark plasma sintering. The nanocomposite samples, with a grain size about 50 nm showed a good mixing and a high density. Their impedance response was measured in the 5 Hz–1 MHz frequency range, under magnetic fields up to 1200 kA/m. Measurements were carried out in the 40–210 °C temperature range. We used the Jonscher's universal relaxation law to analyze the electric conductivity results. Significant changes in the activation energies for long range conductivity and hopping conductivity were observed both at the coercive magnetic field of the ferrite and the Curie transition of the titanate. We show that the use of impedance spectroscopy, based on a wide frequency range, provides a far larger view of electric phenomena allowing a separation of the several contributions to the conductivity phenomena, as a function of the magnetic field.

Index Terms— **Impedance spectroscopy (IS), magnetoelectric effects, nanocomposites.**

I. Introduction

HYBRID nanocomposite materials such as ferrite–ferroelectric phases [1]–[3] are generating a large interest based on their potential applications in a large variety of multifunctional devices like sensors and actuators and magnetoelectric transducers [4]. Since bulk multiferroic materials are scarce, a different approach has been to develop a combination of composite ferro (or ferrimagnetic) and ferroelectric phases. The aim is to obtain a coupling between the two phases and to control the magnetic or electric properties using electric or magnetic fields.

In this paper, we present a study of the electrical properties of $BaTiO_3$–$CoFe_2O_4$ nanocomposites under magnetic fields, at several temperatures. The samples were prepared by a combination of the polyol method [5] to separately synthesize the nanoparticles (NPs) of the two phases, and after mixing to consolidate them by spark plasma sintering (SPS) [6] at relatively low temperatures. This method allows the presence of a high fraction of tetragonal $BaTiO_3$, which possesses a high-electric permittivity. The electric properties were investigated under magnetic field by impedance spectroscopy (IS) [7] in the 5 Hz–1 MHz frequency range. The IS provides a complete image of the electrical phenomena and thus a resolution of the several contributions to the conductivity processes.

II. Experimental Techniques

$BaTiO_3$–$CoFe_2O_4$ nanocomposites were obtained by means of the SPS sintering technique starting from mixed barium titanate ($BaTiO_3$) and cobalt ferrite ($CoFe_2O_4$) NPs, previously synthesized by the polyol method. Structural, electrical, and magnetic characterization, as well as details on the NPs synthesis and SPS procedures can be found elsewhere [8], [9]. Size and morphology of sintered particles were characterized by field emission scanning electron microscopy (FESEM), in a JEOL 7600F microscope. A JEM-9320 focused ion beam (FIB) facility was used to prepare samples for transmission electron microscopy (TEM), performed in a JEOL 1200 EX apparatus operating at 100 kV.

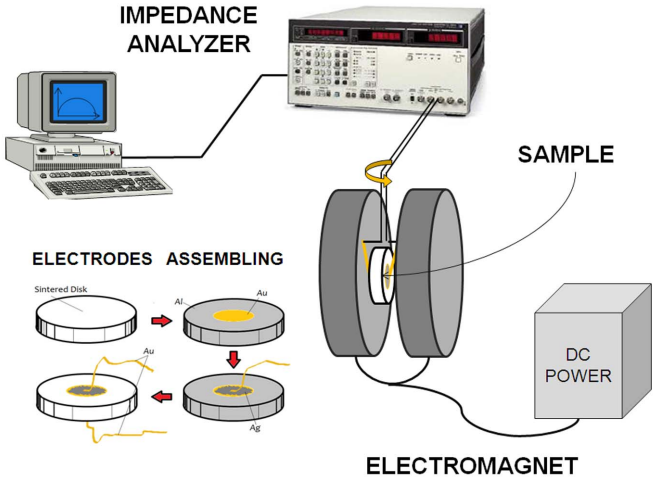

Fig. 1. Experimental configuration of the implemented measurement facility.

Disk shaped sintered samples adapted with parallel gold electrodes over opposite faces were connected to an HP-4192-A impedance analyzer and carefully suited into an electromagnet (Fig. 1). The electromagnet was controlled by a 9600 LDJ VSM magnetometer adapted with a furnace. An ac voltage was applied to the electrodes on both faces (1 V of amplitude); at the same time a constant magnetic field was applied to the sample. Before measuring, the sample was rotated varying the angle between the electric and the magnetic field. Rotation stopped at a fixed position where

Manuscript received March 7, 2014; revised May 6, 2014; accepted May 10, 2014. Date of current version November 18, 2014. Corresponding author: U. A. Salas (e-mail: hydrotier@hotmail.com).

Color versions of one or more of the figures in this paper are available online at http://ieeexplore.ieee.org.

Digital Object Identifier 10.1109/TMAG.2014.2323942

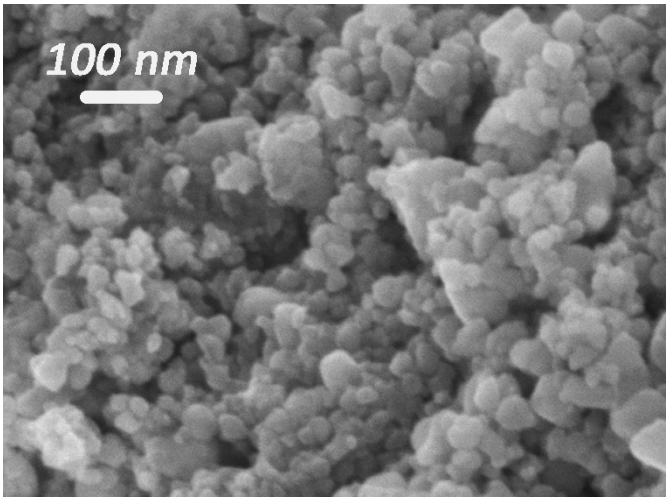

Fig. 2. FESEM micrograph taken on a fracture of the sample.

the complex impedance (directly read from the IS analyzer) reached a maximum value. This value was obtained when a perpendicular configuration of the electrical field with respect to the magnetic was enabled (all data were obtained with this configuration). The ac field frequency was swept from 5 Hz to 1 MHz. Several frequency dependent impedance measurements were carried out in the 40–160 °C range under different magnetic fields (up to 1200 kA/m).

III. Results and Discussion

A. Structural Characterization

The X-ray diffraction patterns of previously studied samples can be found in [8] and [9]. Tetragonal barium titanate and cobalt ferrite phases were confirmed to be present in the studied composites (1/1 molar ratio).

Observations over micrographs taken by FESEM to a fracture on the sample's surface reveal a nano-scaled, homogeneous and random array of the sintered grains, with sizes about 50 nm (Fig. 2). No significant porosity was observed.

A portion of the sintered sample was polished and after ion-milled by FIB. Dark and gray zones can be distinguished on the correspondent micrograph [Fig. 3(a)]. Such contrast on the image can be attributed to a difference on molecular weights. Heavier phases disperse more electrons, so, they look brighter to the detector than lighter phases. Gray zones correspond to cobalt ferrite regions as it is heavier than barium titanate. The inverse criterion can be applied to TEM observations performed over a FIB ion-milled lamella [Fig. 3(b)]. Gray and black grains with sizes below 50 nm are distinguishable. At constant thickness, heavier phases must correspond to dark zones as they absorb more electrons; barium titanate regions must correspond therefore to gray zones and black or dark zones to ferrite (whiter areas represent background).

B. Magnetoelectric Effects and Analysis

The frequency (ω) behavior of the electrical conductivity in a variety of materials is based on the formalism proposed

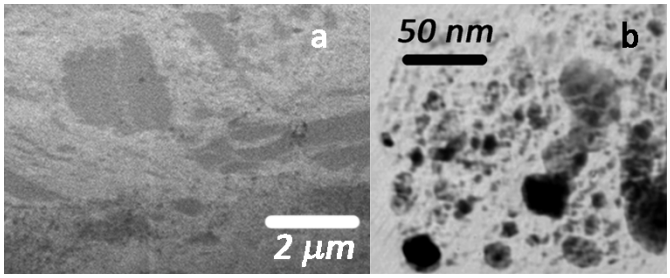

Fig. 3. (a) SEM micrograph of a FIB ion-milled composite sample area. (b) TEM micrograph of a FIB ion-milled lamella (thickness about 100 nm).

in [10], given by a power law

$$\sigma(\omega) = \sigma_{\mathrm{dc}}\left[1 + \left(\frac{\omega}{\omega_H}\right)^n\right] + A\omega \tag{1}$$

where σ_{dc}, ω_H, n, and A are, respectively, the dc (or long range) conductivity, the onset frequency of the ac conductivity (mean frequency of the hopping process), the exponent and the coefficient of the weakly temperature dependent term. The first and the second terms in (1) refer to the universal dielectric response and to the nearly constant loss, respectively.

The temperature dependence of the dc conductivity and the hopping frequency follows an Arrhenius dependence

$$\sigma_{\mathrm{dc}} T = \sigma_0 \exp\left(\frac{-U_{\mathrm{dc}}}{K_B T}\right) \tag{2}$$

$$\omega_H = \omega_0 \exp\left(\frac{-U_H}{K_B T}\right) \tag{3}$$

U_{dc} and U_H are the activation energies for dc conductivity and the hopping frequencies for the carriers, respectively, σ_0 and ω_0 are pre-exponential factors.

Results for frequency dependent conductivity measurements at several temperatures and four different applied magnetic fields (from 0 to 716 kA/m) are shown in Fig. 4. All experimental curves show a good agreement with (1). Modeling is very good; its solid lines are barely visible behind the experimental points. These results enabled us to go further on the modeling.

Using (2) and (3), a calculation of activation energies for the composite was carried out, leading to linear modeling, as shown in Fig. 5. A good agreement can be observed. The conductivity parameters determined for each fitting are shown in inset. Arrhenius plots for the dc conductivity activation energy (U_{dc}) are shown in column a, and those for hopping activation energy (U_H) appear in column b (Fig. 5).

A change of slope in both parameters, U_{dc} and U_H, can be observed for temperatures near the well known barium titanate Curie transition ($T_C \approx 120$ °C), pointing to a different conductivity mechanism when ferroelectric ordering vanishes (Fig. 5). In the absence of magnetic field, the long range conductivity is independent of the ferroelectric order. However, when magnetic field is applied, the ferroelectric phase is influenced by the magnetic order in ferrite NPs, leading to a change in both dc and hopping conductivities.

In contrast, the process responsible for charge hopping conductivity is sensitive to the ferroelectric order regardless of magnetic fields. This suggests that the energy needed for

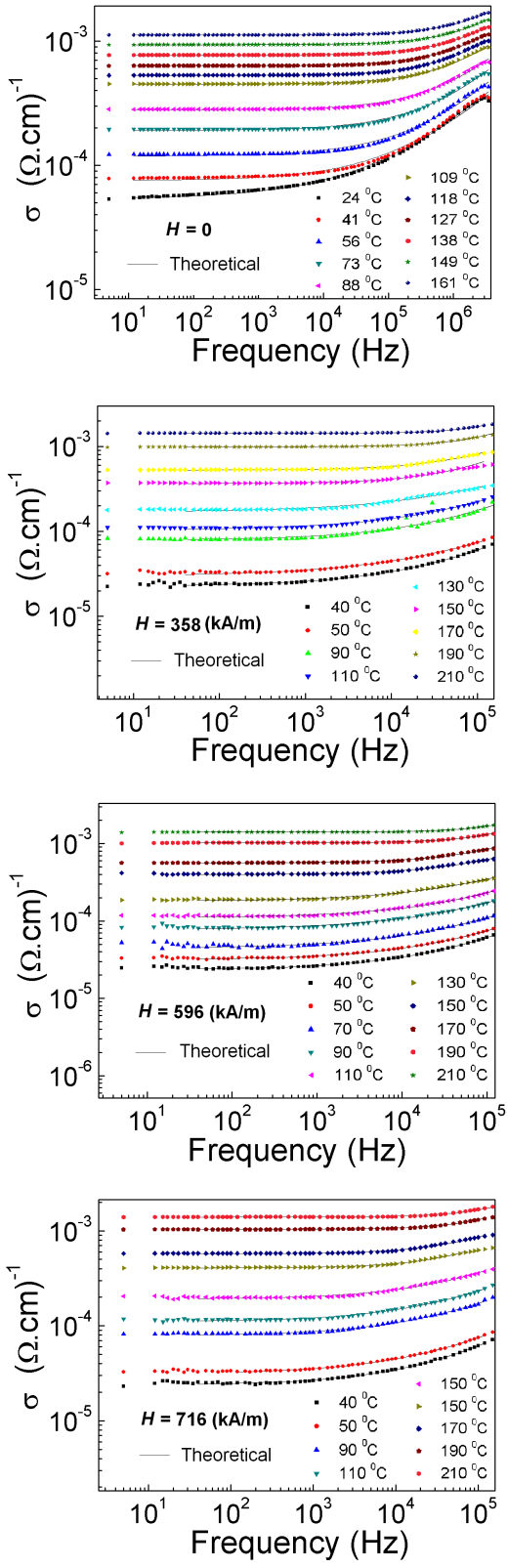

Fig. 4. Frequency dependent conductivity at several temperatures and four different magnetic fields.

hopping process has two different contributions, one from ferrimagnetic NPs and the other from the ferroelectric ones.

Below barium titanate T_C, the activation energy for hopping process (U_H) decreases when magnetic field is applied,

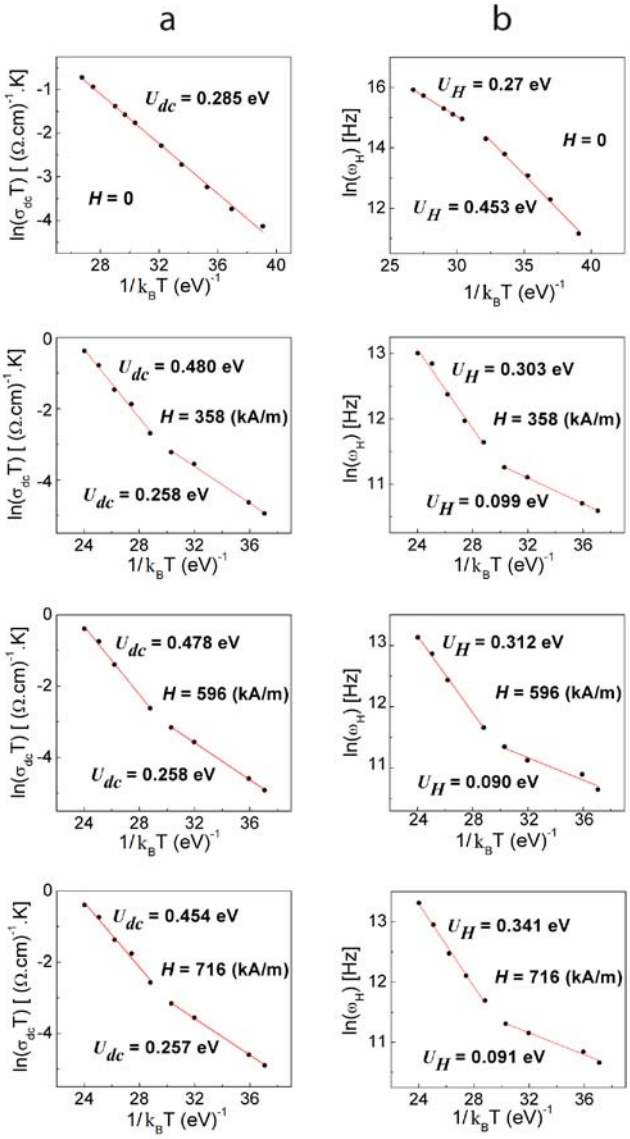

Fig. 5. (a) Arrhenius plots for dc conductivity under four different applied magnetic fields. (b) Arrhenius plots for hopping frequency under four different applied magnetic fields.

whereas activation energy for long range conductivity (U_{dc}) shows no change (Fig. 6). It is important to note that at zero magnetic field the species involved on hopping phenomena are oxygens migrating within ferroelectric particles, as shown previously in ABO_3 perovskite-type oxides [11], [12]. When a magnetic field higher than the ferrimagnetic coercive field is applied the hopping species changes to electrons, as the correspondent activation energy value suggest [13]. Thus, activation energy for hopping process decreases when magnetic field is applied in spite that the charge transport species involved on hopping mechanism changes from less to more conductive species.

Activation energy value for hopping conductivity below T_C decreases from 0.45 to 0.09 eV when magnetic field is applied (above the coercive field). The 0.45 eV value at zero magnetic field can be associated with oxygen's first ionization process [11], [12] and the 0.09 eV is associated to electronic transfer between Fe^{2+}, Co^{2+}, and Fe^{3+} species [13]. The latter

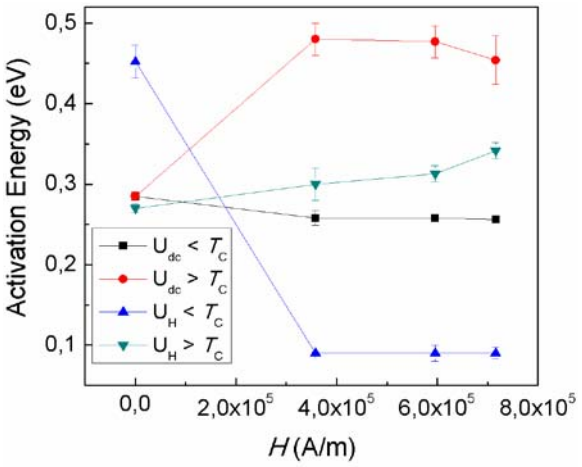

Fig. 6. Activation energy for dc conductivity and hopping frequency versus magnetic field.

evidence shows that hopping charge transport is improved by magnetic field when barium titanate is ferroelectric. This could be a consequence of a coupling between spontaneous electric dipoles in ferroelectric particles, and their spontaneous magnetic counterparts. As we demonstrated before, the dilution of the ferrimagnetic NPs by the diamagnetic $BaTiO_3$ NPs leads to a more defined single domain behavior [9], increasing the local magnetostatic field. The interaction of this magnetostatic field with the local electric field in ferroelectric particles can be expected to be the source of the observed coupling. The phase changes both of ferromagnetic and ferroelectric NPs at the nanoscale have an effect on the hopping activation energy at the macroscale.

Below barium titanate T_C, long-range conductivity is insensitive to the applied magnetic field. Above T_C its activation energy increases with magnetic field. Therefore, the absence of ferroelectric order makes long-range charge transport more difficult if a magnetic field is applied (Fig. 6).

Observed changes exhibited a relationship with the composite coercive field ($H_c = 121$ kA/m [9]). When the applied magnetic field exceeds this value all conduction processes seem to achieve stability. In contrast, when the system is perturbed with a magnetic field near to the coercive value, pronounced changes are promoted on charge transport behavior. At this value of field, all the magnetic particles are randomly oriented, as net magnetization is zero. Near saturation, the magnetization of all magnetic NPs is aligned with the field direction. These drastic changes in magnetic structure modify the different electric conduction processes in the composite.

IV. Conclusion

In this paper, we showed that the use of IS, based on a wide frequency range, provides a far larger view of electric phenomena allowing a separation of several contributions to the conductivity processes, as a function of the applied magnetic field.

Apparent changes in different charge transport phenomena were observed (via the correspondent activation energies) near the T_C of the ferroelectric phase and near the composite magnetic coercive field. Hopping conductivity processes change near T_C regardless of the magnetic field; below T_C, such transport mechanism can be improved by applying a magnetic field. Long range conductivity processes change near T_C only under magnetic field.

Presented results give indication of a strong coupling between the magnetic structures of cobalt ferrite NPs with the spontaneously polarized ferroelectric structure of barium titanate NPs, through the electrical behavior on the studied system.

Acknowledgment

This work was supported by the Agence Nationale de la Recherché—CONACyT, México, under Project 139292 and Project PAPIIT-IN 141012. The work of R. L. Noda was supported by the Centro Latinoamericano de Física for the Co- Operative Grant. The authors would like to thank C. Flores and J. Arellano for the contribution to FIB and TEM techniques.

References

[1] W. Chen, W. Zhu, X. F. Chen, and L. L. Sun, "Preparation of $(Ni_{0.5}Zn_{0.5})Fe_2O_4/Pb(Zr_{0.53}Ti_{0.47})O_3$ thick films and their magnetic and ferroelectric properties," *Mater. Chem. Phys.*, vol. 127, nos. 1–2, pp. 70–73, 2011.

[2] C. H. Sim, A. Z. Z. Pan, and J. Wang, "Thickness and coupling effects in bilayered multiferroic $CoFe_2O_4/Pb(Zr_{0.53}Ti_{0.47})O_3$ thin films," *J. Appl. Phys.*, vol. 103, no. 12, pp. 124109-1–124109-7, Jun. 2008.

[3] J.-P. Zhou, H. He, Z. Shi, and C.-W. Nan, "Magnetoelectric $(Ni_{0.5}Zn_{0.5})Fe_2O_4/Pb(Zr_{0.52}Ti_{0.48})O_3$ double-layer thin film prepared by pulsed-laser deposition," *Appl. Phys. Lett.*, vol. 88, no. 1, p. 013111, Jan. 2006.

[4] N. A. Spaldin and M. Fiebig, "The renaissance of magnetoelectric multiferroics," *Science*, vol. 309, no. 5733, pp. 391–392, 2005.

[5] M. Artus *et al.*, "Synthesis and magnetic properties of ferrimagnetic $CoFe_2O_4$ nanoparticles embedded in an antiferromagnetic NiO matrix," *Chem. Mater.*, vol. 20, no. 15, pp. 4861–4872, 2008.

[6] R. Orrù, R. Licheri, A. M. Locci, A. Cincotti, and G. Cao, "Consolidation/synthesis of materials by electric current activated/assisted sintering," *Mater. Sci. Eng. R, Rep.*, vol. 63, nos. 4–6, pp. 127–287, Feb. 2009.

[7] J. R. Macdonald and W. R. Kenan, *Impedance Spectroscopy: Emphasizing Solid Materials and Physics*. New York, NY, USA: Wiley, 1987.

[8] U. Acevedo, T. Gaudisson, R. López-Noda, S. Ammar, S. Nowak, and R. Valenzuela, "Electrical properties of $CoFe_2O_4$-$BaTiO_3$ nanostructured composites prepared by a combination of chimie douce and spark plasma sintering," *J. Spintronics Magn. Nanomater.*, vol. 1, no. 2, pp. 85–90, Aug. 2012.

[9] U. Acevedo, R. Ortega, R. Valenzuela, T. Gaudisson, S. Ammar, and S. Nowak, "Magnetic properties of ferrite-titanate nanostructured composites synthesized by the polyol method and consolidated by spark plasma sintering," *J. Appl. Phys.*, vol. 113, no. 17, p. 17B519, 2013.

[10] A. K. Jonscher, *Dielectric Relaxation in Solids*. London, U.K.: Chelsea Dielectrics Press, 1983.

[11] M. S. Islam, "Ionic transport in ABO_3 perovskite oxides: A computer modelling tour," *J. Mater. Chem.*, vol. 10, no. 4, pp. 1027–1038, 2000.

[12] A. Peláiz-Barranco and R. López-Noda, "Dielectric relaxation and electrical conductivity in ferroelectric ceramic/polymer composite based on modified lead titanate," *J. Appl. Phys.*, vol. 102, no. 11, p. 114102, Dec. 2007.

[13] E. J. Verwey, P. W. Haayman, and F. C. Romeijn, "Physical properties and cation arrangement of oxides with spinel structures II. Electronic conductivity," *J. Chem. Phys.*, vol. 15, no. 4, pp. 181–187, 1947.